MCB
Journals.ASM.org

Histone ADP-Ribosylation Facilitates Gene Transcription by Directly Remodeling Nucleosomes

Ricardo Martinez-Zamudio and Hyo Chol Ha

Department of Biochemistry and Molecular & Cellular Biology, Georgetown University Medical Center, Washington, DC, USA

The packaging of DNA into nucleosomes imposes obstacles on gene transcription, and histone-modifying and nucleosome-remodeling complexes work in concert to alleviate these obstacles so as to facilitate transcription. Emerging evidence shows that chromatin-associated poly(ADP-ribose) polymerase 1 (PARP-1) and its enzymatic activity facilitate inflammatory gene transcription and modulate the inflammatory response in animal models. However, the molecular mechanisms by which PARP-1 enzymatic activity facilitates transcription are not well understood. Here we show that through an intracellular signaling pathway, lipopolysaccharide (LPS) stimulation induces PARP-1 enzymatic activity and the ADP-ribosylation of histones at transcriptionally active and accessible chromatin regions in macrophages. *In vitro* DNase I footprinting and restriction endonuclease accessibility assays reveal that histone ADP-ribosylation directly destabilizes histone-DNA interactions in the nucleosome and increases the site accessibility of the nucleosomal DNA to nucleases. Consistent with this, LPS stimulation-induced ADP-ribosylation at the nucleosome-occupied promoters of *il-1*β, *mip-2*, and *csf2* facilitates NF-κB recruitment and the transcription of these genes in macrophages. Therefore, our data suggest that PARP-1 enzymatic activity facilitates gene transcription through increasing promoter accessibility by histone ADP-ribosylation.

Poly(ADP-ribose) polymerase 1 (PARP-1) is a chromatin-associated enzyme. In response to DNA strand breaks, activated PARP-1 hydrolyzes NAD^+ and transfers ADP-ribose units successively to itself and other target proteins, including histones (24). Poly(ADP-ribose) (pADPr) is a homopolymer of ADP-ribose units and a posttranslational protein modifier (11). Recently, the enzymatic activity of PARP-1 has been implicated in the regulation of NF-κB-dependent inflammatory gene expression (17, 20, 24, 42, 45). In addition, inhibition of PARP-1 enzymatic activity significantly reduces neutrophil infiltration in animal models of carrageenan-induced edema, allergic encephalomyelitis, and zymosan-induced multiple-organ failure (14, 56), suggesting that the synthesis of ADP-ribose plays a role in the inflammatory response. Accordingly, glia and macrophages treated with PARP inhibitors display defective lipopolysaccharide (LPS)-induced gene expression (42). Consistent with studies of PARP inhibitors, PARP-1-deficient mice are resistant to LPS stimulation-induced endotoxic shock (46). Moreover, we have shown previously that primary glia derived from PARP-1-deficient mice display defective LPS stimulation-induced gene expression, due in part to a lack of transcription factor activation (16, 17). However, despite accumulating evidence that PARP-1 facilitates gene transcription, the molecular mechanisms by which PARP-1 and its enzymatic activity facilitate gene transcription are not well understood at present.

Nucleosomes are the basic repeating unit of chromatin, creating barriers to factors requiring access to DNA (34). Particularly, the interactions between histones and DNA in the nucleosome pose a challenge for several steps of the transcription process, including activator binding, preinitiation complex assembly, and elongation (60). Accordingly, the cell has developed highly regulated mechanisms to alleviate these structural constraints so as to facilitate transcription, including the ATP-dependent chromatin-remodeling complexes in concert with histone posttranslational modifications (PTMs) (8, 27). For instance, the NURF and SWR1 ATP-dependent chromatin-remodeling complexes have been shown to catalyze the sliding of the histone octamer along DNA and the exchange of the histone H2A variant H2AZ, respectively, to facilitate transcription (18, 19, 40).

Histone PTMs facilitate transcription primarily by acting as binding platforms for *trans*-acting factors, including ATP-dependent chromatin remodelers. This is exemplified by H3K4 trimethylation- and H4 acetylation-dependent recruitment of chromatin-remodeling complexes and general transcription factors to the promoters of genes (23, 63). In addition, histone H4K16 acetylation has been shown to regulate the higher-order chromatin structure by promoting the unfolding of nucleosome arrays *in vitro* (55). However, the 10- to 11-bp DNA helical repeat and the hydrodynamic properties of hyperacetylated nucleosomes (>12 acetates per octamer) are nearly identical to those of unmodified nucleosomes (5), indicating that histone acetylation may not alter histone-DNA interactions in individual nucleosomes (48). Currently, it is not well understood whether a histone PTM alone can directly regulate histone-DNA interactions in individual nucleosomes (4, 52).

To better understand the molecular mechanisms by which PARP-1 enzymatic activity facilitates gene transcription, we investigated the targets and the role of ADP-ribosylation in LPS stimulation-inducible inflammatory gene transcription in macrophages. In this report, we show that LPS stimulation induces histone ADP-ribosylation at transcriptionally active and accessible chromatin regions in macrophages. *In vitro* DNase I hypersensitivity and restriction endonuclease accessibility assays show that histone ADP-ribosylation alters histone-DNA interactions in the

Received 5 December 2011 **Returned for modification** 9 January 2012
Accepted 17 April 2012
Published ahead of print 30 April 2012
Address correspondence to Hyo Chol Ha, mcj22@georgetown.edu.

doi:10.1128/MCB.06667-11

nucleosome and increases the accessibility of nucleosomal DNA. Consistent with this, chromatin immunoprecipitation (ChIP) analyses show that LPS stimulation-induced ADP-ribosylation facilitates NF-κB recruitment to *il-1*β, *mip-2*, and *csf2* promoters and that inhibition of ADP-ribosylation significantly reduces the transcription of these genes in LPS-stimulated macrophages. Collectively, the data indicate that PARP-1 enzymatic activity facilitates efficient gene transcription through increasing the accessibility of the promoter regions by histone ADP-ribosylation.

MATERIALS AND METHODS

Antibodies and reagents. Anti-PARP-1 (H250), anti-NF-κB p65 (C20), and protein A/G beads were purchased from Santa Cruz Biotechnologies. Anti-phospho-IκBα (5A5), anti-extracellular signal-regulated kinase (anti-ERK) (137F5), and anti-phospho-ERK (D13.14.4E) were from Cell Signaling Technologies. Anti-histone H3 (1791) was from Abcam. Anti-H2B (AB1623), anti-acetylated H3 (anti-AcH3) (06-599), anti-phospho-H2AX (07-164), anti-p38 mitogen-activated protein kinase (anti-p38 MAPK) (341-360), anti-phospho-p38α (AB3828), and streptavidin agarose were from Millipore. Anti-pADPr (LP-9610) was from Alexis. LPS from *Salmonella enterica* serotype Typhimurium, micrococcal nuclease (MNase) from *Staphylococcus aureus*, IMD-0354, and anti-actin (C5838) were from Sigma. PJ34 was from Alexis Biochemicals. ADP-HPD, SB203580, and UO126 were from Calbiochem. The protease inhibitor cocktail was from Roche.

Tissue culture. RAW 264.7 macrophages were cultured in Dulbecco's modified Eagle medium (DMEM) supplemented with 10% fetal bovine serum (FBS) and 0.1 U/ml penicillin–0.1 μg/ml streptomycin at 37°C. For measurements of PARP enzymatic activity, cells were cultured with 0.5% FBS overnight before stimulation with LPS. Primary glial cells isolated from PARP-1 wild-type and knockout mice were cultured as described previously (17).

PARP enzymatic activity assay. The PARP enzymatic activity assay was performed as described previously (17) with some modifications. Cells stimulated with LPS (1 μg/ml) were carefully harvested and were isolated by centrifugation (800 × *g*, 3 min, 4°C). The cell pellet was gently resuspended in PARP assay buffer containing 50 mM Tris-HCl (pH 8.0), 28 mM KCl, 10 mM $MgCl_2$, 0.01% digitonin, 1 mM dithiothreitol (DTT), and ^{32}P-NAD$^+$ (0.5 μCi/10^6 cells, 0.8 μCi/nmol [1 Ci = 37 GBq]) for 20 min at 4°C. The reaction was stopped by adding the PARP and poly(ADP-ribose) glycohydrolase (PARG) inhibitors PJ34 (10 μM) and ADP-HPD (500 nM), respectively. After centrifugation, cells were either lysed as described below or subjected to small-scale biochemical fractionation as described below. Equal amounts of protein were separated on 4-to-12% or 12% NuPAGE gels (Invitrogen) and were transferred to nitrocellulose membranes. PARP enzymatic activity was visualized by autoradiography.

Preparation of cell lysates. Cells were broken in lysis buffer containing 100 mM HEPES (pH 7.4), 100 mM NaF, 0.5% NP-40, 40 mM EDTA, 4 mM EGTA, 150 mM NaCl, 10 μM PJ34, 500 nM ADP-HPD, and a protease inhibitor cocktail for 30 min with vortexing (10 s for every 10 min). The lysates were cleared by centrifugation (12,000 × *g*, 15 min, 4°C), and the supernatant (S1) was collected. For analysis of histones and other chromatin-associated proteins, the insoluble pellet (P1) was extracted with 0.4 N HCl or was solubilized in sodium dodecyl sulfate (SDS) lysis buffer (1% SDS, 20 mM Tris-HCl [pH 8.0], 2 mM EDTA) by sonication with a Branson sonifier, model 250, equipped with a model 102C tip (40% output; 4 times for 10 s).

Small-scale biochemical fractionation. Small-scale biochemical fractionation was performed as described previously (61) with some modifications. Briefly, 10^7 cells were collected, washed with ice-cold phosphate-buffered saline (PBS), and resuspended in buffer A containing 10 mM HEPES (pH 7.4), 10 mM KCl, 1.5 mM $MgCl_2$, 0.34 M sucrose, 10% glycerol, 1 mM DTT, 0.1 mM phenylmethylsulfonyl fluoride (PMSF), 10 μM PJ34, 500 nM ADP-HPD, and a protease inhibitor cocktail. Triton X-100 was added (final concentration, 0.1%); the cells were incubated on ice for 5 min; and nuclei (P1) were collected by centrifugation (1,300 × *g*, 4 min, 4°C). The nuclei were lysed for 10 min on ice in hypotonic buffer B containing 3 mM EDTA, 0.2 mM EGTA, 1 mM DTT, 10 μM PJ34, 500 nM ADP-HPD, and the protease inhibitor cocktail. The chromatin (P3) and soluble nuclear (S3) fractions were separated by centrifugation (1,700 × *g*, 4 min, 4°C). The P3 fraction was resuspended in buffer C, containing 10 mM Tris-HCl (pH 7.5), 10 mM KCl, 1 mM $CaCl_2$, 10 μM PJ34, and 500 nM ADP-HPD, and was digested with MNase at a final concentration of 2.5 U/ml for 10 min (for native chromatin) or 40 U/ml (for cross-linked chromatin) at 37°C for the indicated times (see Fig. 4). The reaction was stopped by the addition of 1 mM EGTA, and the soluble chromatin fraction (S4) was obtained by centrifugation (1,700 × *g*, 5 min, 4°C). Alternatively, the P3 fraction was resuspended in SDS lysis buffer and was sonicated with a Branson sonifier, model 250, equipped with a model 102C tip (40% output; 4 times for 10 s). Soluble chromatin was obtained by centrifugation (12,000 × *g*, 15 min, 4°C).

Real-time reverse transcription-PCR. For gene expression analysis, RNA was extracted with the RNeasy kit (Qiagen) according to the manufacturer's instructions. RNA (1 μg) was reverse transcribed using TaqMan reverse transcription reagents (Applied Biosystems) according to the manufacturer's instructions. Real-time PCR was performed with SYBR green PCR Master Mix (Applied Biosystems) in an ABI Prism 7500 real-time system (Applied Biosystems). Primers are available upon request.

ChIP. Control and LPS-stimulated RAW 264.7 macrophages were cross-linked with 0.5% formaldehyde in PBS for 8 min at room temperature. The reaction was quenched by addition of 125 mM glycine for 8 min at room temperature, and the cells were collected by centrifugation (800 × *g*, 3 min, 4°C). The cells were subjected to small-scale biochemical fractionation as described above, except that the final concentration of MNase was 40 U/ml. The average size of chromatin was 1 to 5 nucleosomes. Chromatin was diluted 10-fold in chromatin immunoprecipitation (ChIP) dilution buffer containing 1.1% Triton X-100, 0.1% SDS, 167 mM NaCl, 22.3 mM Tris-HCl (pH 8.0), and 2.2 mM EDTA and precleared with 30 μl of a 50% protein A/G agarose slurry for 2 h at 4°C. Immunoprecipitation was performed using 2 μg of anti-PARP-1, anti-NF-κB p65, and anti-histone H3 antibodies. Isotype-matched IgG and a mock precipitation without antibodies were used as negative controls for immunoprecipitation. After isolation of the immune complexes by incubation with protein A/G beads overnight at 4°C, the beads were collected by centrifugation. The beads were washed 3 times with a wash buffer containing 1% Triton X-100, 0.1% SDS, 150 mM NaCl, 20 mM Tris-HCl (pH 8.0), and 2 mM EDTA, once with a wash buffer containing 300 mM NaCl, and twice with Tris-EDTA (TE) buffer (pH 8.0). Immune complexes were eluted twice with an elution buffer containing 1% SDS and 100 mM sodium acetate (NaOAc) at 37°C. After reversal of cross-links (4 h, 65°C), the samples were treated with proteinase K and RNase A (500 μg/ml each, 1 h, 42°C), and DNA was purified by phenol-chloroform extraction followed by ethanol (EtOH) precipitation. DNA was resuspended in TE, and 1/20 of the recovered DNA was used for PCRs (30 to 32 cycles). For biotinylated-NAD$^+$ ChIP experiments, the procedure was carried out identically except that cells were labeled with 50 μM biotinylated NAD$^+$ as described under "PARP enzymatic activity assay" above, and ADP-ribosylated complexes were isolated with streptavidin-coupled agarose beads. Input DNA and PCR products were analyzed in 1.5% Tris-borate-EDTA (TBE) agarose gels and were visualized by SYBR green staining. Primers are available upon request.

Sucrose gradient analysis of MNase-digested chromatin. For sucrose gradient sedimentation analyses, 10-to-40% sucrose gradients were prepared in TE buffer containing 150 mM NaCl. The total volume of the gradient was 3.5 ml. The S4 fraction (200 μl) from untreated and LPS-stimulated macrophages was layered carefully on the top of the gradient and was centrifuged at 32,000 rpm for 16 h at 4°C in an SW50.1 rotor. Fractions (250 μl) were collected from the bottom of the tube. Fractions (10%) were directly analyzed by SDS-polyacrylamide gel electrophoresis

(PAGE). For DNA analysis, 10% of each fraction was aliquoted, and protein was digested by addition of 10 mg/ml proteinase K (New England Biolabs [NEB]) for 1 h at 37°C. DNA was purified by phenol-chloroform extraction and was precipitated with EtOH for 1 h at −80°C. After centrifugation (30 min, 4°C), the DNA pellet was washed once with 70% EtOH and was allowed to dry in the fume hood. DNA was analyzed by agarose gel electrophoresis and was visualized by ethidium bromide staining.

Mononucleosome assembly. Mononucleosomes were assembled by stepwise dilution from 2 M NaCl (36). Briefly, the 168- and 282-bp DNA fragments of the 601 nucleosome positioning sequence (37) and the rDNA murine promoter (−232, +16) (32) were amplified by PCR and were gel purified using the Qiagen gel extraction kit. Purified DNA fragments (5 μg) were incubated with chicken core histones (ratio, 1:1.4 by weight) in a 100-μl reaction mixture in the presence of 2 M NaCl and 100 ng bovine serum albumin (BSA) for 3 h at 37°C. Low-salt buffer (20 mM Tris-HCl [pH 7.5], 100 μg/ml BSA, 1 mM EDTA, 0.5 mM PMSF, 5 mM DTT) was slowly added in volumes of 100, 200, 400, and 600 μl with 60-min incubations after each addition. The assembled nucleosomes were assessed by native gel electrophoresis by adding 10% glycerol and loading onto 1% agarose gels prepared in 0.2× TBE and were analyzed at 50 V in 0.2× TBE for 1 h at room temperature. The corresponding DNA fragments were analyzed simultaneously in the gel as a reference. DNA was stained with SYBR green and was visualized in a UV transilluminator. The concentration of each nucleosome preparation was determined by comparing the SYBR green signal intensities of an aliquot of each preparation and a known amount of each of the DNA fragments used for assembly.

Generation of pADPr-PARP-1. Recombinant PARP-1 (1 μg) was incubated in 100-μl reaction mixtures containing 0.2, 2, and 20 μM NAD^+ and a 1 μM concentration of a 25-base single-stranded oligonucleotide in the presence of 1.5 mM $MgCl_2$. The reaction was allowed to proceed for 20 min at room temperature and was then stopped with 1 mM PJ34. Poly(ADP-ribosyl)ated PARP-1 (pADPr-PARP-1) was purified by centrifugation in a Microcon concentrator (10,000-Da cutoff; Millipore) according to the manufacturer's instructions. Purified pADPr-PARP-1 was diluted in 10 μl low-salt buffer at a concentration of 100 ng/μl.

Nucleosome-remodeling assay. For poly(ADP-ribosyl)ation-dependent nucleosome-remodeling reactions, recombinant PARP-1 was incubated with assembled nucleosomes (PARP-1/nucleosome molar ratio, 2:1; we typically used ~0.4 to 0.8 pmol nucleosomes) in 20-μl reaction mixtures in the presence of 1.5 mM $MgCl_2$ and 150 mM NaCl for 5 min at room temperature. A 100 mM NAD^+ stock solution was prepared in low-salt buffer. In order to add the same volume of NAD^+ to each reaction mixture, we serially diluted NAD^+ down to 1 μM in low-salt buffer. NAD^+ was then added to the concentrations indicated in Fig. 5 and 6 (also data not shown), and the reactions were allowed to proceed for 20 min at room temperature. The PARP inhibitor PJ34 was then added to a final concentration of 1 mM. For PARP-1 binding reactions, the same molar ratio was maintained, and the reaction was allowed to proceed for 30 min at room temperature. All reactions were quenched on ice for 5 min prior to analysis by native agarose gel electrophoresis.

Restriction endonuclease accessibility assay. Nucleosomes were assembled with the 282-bp fragment of the 601 nucleosome positioning sequence (37) and the 248-bp rDNA promoter DNA fragment (32). Control nucleosomes and nucleosomes incubated with PARP-1 and NAD^+ as described above were digested with 50 U of the StyI or HaeIII enzyme in their respective NEB buffers for 1.5 h at 37°C. Reactions were analyzed by electrophoresis in a 1.7% native agarose gel, followed by SYBR green staining, and products were visualized in a UV transilluminator.

DNase I hypersensitivity and ExoIII mapping of nucleosome positions. The 601 nucleosome positioning sequence (37) was labeled with ^{32}P at the 5′ end of the sense or antisense strand during the PCR step, and nucleosomes were reconstituted with the labeled sequence as described above. Control and remodeled nucleosomes were then digested with 5 U of DNase I (NEB) in 1× DNase I buffer (NEB) for 30 s at room temperature. Naked DNA was digested with 0.5 U of DNase I. For exonuclease III (ExoIII) mapping experiments, control and remodeled nucleosomes were digested with 1,000 U/ml of ExoIII for 15 min at 37°C in NEB buffer 1. Naked DNA was digested for 1 min. Digestions were quenched by addition of 10 mM EDTA. Protein was digested by addition of 10 mg/ml proteinase K (NEB) for 1 h at 37°C. Unlabeled carrier DNA (5 μg) was then added to the reaction mixtures. DNA was purified by two phenol-chloroform extractions and was precipitated with EtOH for 1 h at −80°C. After centrifugation (30 min, 4°C), the DNA pellet was washed once with 70% EtOH and was allowed to dry in the fume hood. DNA was resuspended in formamide buffer (95% [vol/vol] formamide, 10 mM EDTA [pH 8.0], 0.1% [wt/vol] bromophenol blue, 0.1% [wt/vol] xylene cyanol), boiled for 5 min at 95°C, and separated in a denaturing sequencing gel (1× TBE, 8% polyacrylamide, 8 M urea). Gels were visualized by autoradiography.

RESULTS

LPS stimulation induces poly(ADP-ribosyl)ation of PARP-1. To better understand the role of ADP-ribose synthesis in inflammatory gene transcription, we sought to characterize the enzymatic activity of PARP-1 in macrophages. To this end, we performed the PARP enzyme assay utilizing ^{32}P-NAD^+ for labeling LPS stimulation-specific *de novo* ADP-ribose synthesis. Surprisingly, we found that LPS stimulation increased the level of [^{32}P]pADPr-PARP-1 over the basal level in a time-dependent manner (Fig. 1A and B). Consistent with this result, immunoblot analysis with antibodies against poly(ADP-ribose) showed a time-dependent increase in the level of the ADP-ribose polymer, which was synthesized from the endogenous NAD^+, in response to LPS stimulation (Fig. 1C). Furthermore, PARP-1 immunoprecipitated by an antibody against PARP-1 from nuclear extracts of ^{32}P-NAD^+-labeled macrophages was modified with LPS stimulation-induced [^{32}P]poly(ADP-ribose) (Fig. 1D). Together, these results indicate that LPS stimulation induces PARP-1 enzymatic activity.

PARP-1 is a chromatin-associated protein. We then determined the regions where PARP-1 enzymatic activity was induced by LPS stimulation in macrophages. Micrococcal nuclease (MNase) digestion can reveal nucleosome occupancy and position by preferentially cutting linker DNA between nucleosomes (31). We therefore performed MNase digestion after classical biochemical fractionation (Fig. 1E). DNA analysis showed chromatin-free soluble nuclear (S3), MNase-accessible chromatin (S4), and MNase-resistant chromatin (P4) fractions (Fig. 1F). Immunoblot analysis of these fractions revealed that PARP-1 was distributed in all three fractions (Fig. 1F). Interestingly, LPS stimulation-induced [^{32}P]pADPr-PARP-1 was enriched in the S3 and S4 fractions but barely detectable in the P4 fraction, despite similar PARP-1 protein levels (Fig. 1F). In addition, [^{32}P]pADPr-PARP-1 was completely absent from the S3 fraction generated after cross-linking of chromatin from ^{32}P-NAD^+-labeled macrophages (Fig. 1G), suggesting that the presence of [^{32}P]pADPr-PARP-1 in the S3 fraction is likely a result of release from chromatin or partial association with chromatin. Pretreatment of cells with the PARP inhibitor PJ34 abrogated the LPS stimulation-induced poly(ADP-ribosyl)ation of PARP-1 (Fig. 1F). Together, these results suggest that LPS stimulation-induced PARP-1 enzymatic activity occurs at chromatin.

LPS stimulation induces histone ADP-ribosylation through an intracellular signaling pathway. Histone modifications induced by transcriptional stimuli facilitate gene transcription (54, 62), and chromatin-associated PARP-1 may target histones with

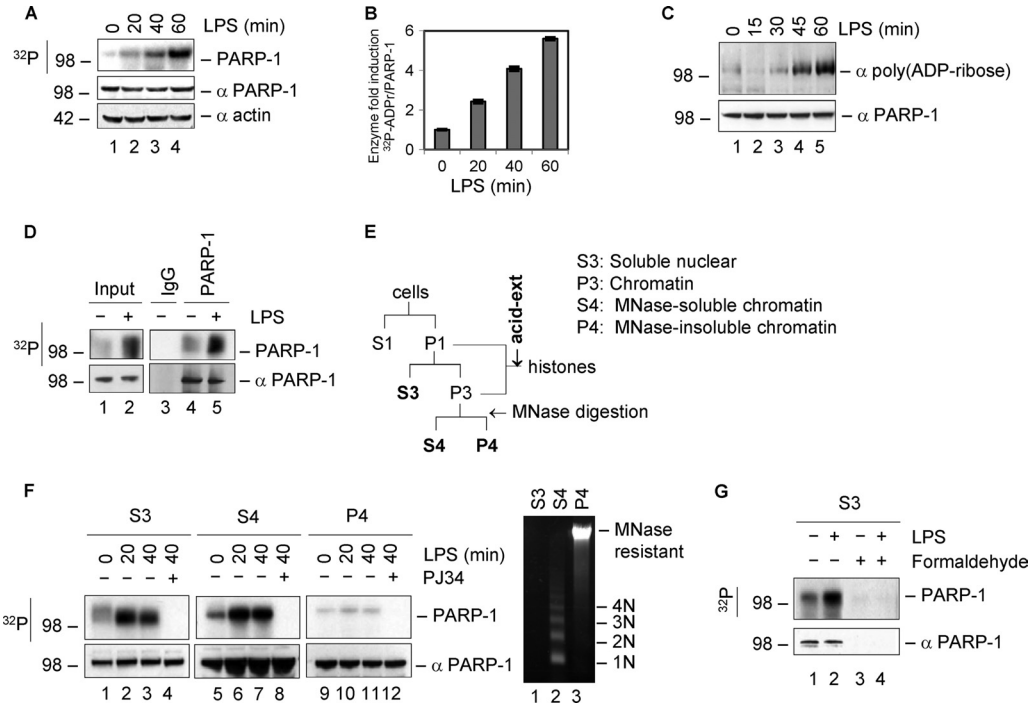

FIG 1 LPS stimulation induces PARP-1 enzymatic activity. (A) RAW 264.7 macrophages were stimulated with LPS for the indicated times. Immediately after the PARP enzymatic assay, protein was extracted with a nonionic detergent, separated by NuPAGE gels, and transferred to nitrocellulose membranes. [^{32}P]pADPr-PARP-1 was detected by autoradiography (A, D, F, and G). (B) Semiquantitative analysis of LPS stimulation-induced PARP-1 enzymatic activity. Fold inductions were determined as the ratio of the ^{32}P signal over PARP-1 protein levels and are relative to levels in unstimulated cells (0 min). Results are from at least three independent experiments performed as described for panel A. Data are means ± standard errors of the means. (C) The endogenous ADP-ribose polymer was detected in LPS-stimulated macrophages by Western blot analysis with antibodies to poly(ADP-ribose). (D) PARP-1 was immunoprecipitated with antibodies against PARP-1 from nuclear extracts from control and LPS-stimulated macrophages. IgG was used as a negative control. (E) Biochemical fractionation scheme. Fractions analyzed in this study are in boldface. (F) (Left) Cells were stimulated with LPS and were processed as for panel A. Subsequently, cells were subjected to biochemical fractionation in order to determine the distribution of PARP-1 and pADPr-PARP-1 in the S3, S4, and P4 fractions. PJ34 is a PARP inhibitor. (Right) DNA analysis shows biochemical fractionation of the S3, S4, and P4 fractions. N, number of nucleosomes. (G) Control and LPS-stimulated macrophages were fixed with or without formaldehyde immediately after the PARP enzymatic assay. After biochemical fractionation, the S3 fractions were analyzed. LPS and PJ34 were used at concentrations of 1 μg/ml and 10 μM, respectively, throughout the study.

ADP-ribose in LPS-stimulated macrophages. We therefore determined the level of histone ADP-ribosylation by analyzing acid-soluble histones prepared from the nuclei of ^{32}P-NAD$^+$-labeled macrophages (Fig. 1E). LPS stimulation significantly increased the levels of [^{32}P]ADP-ribosylated histones (ADPr-histones) over the basal levels in resting cells in a time-dependent manner (Fig. 2A and B). Pretreatment of macrophages with PJ34 abrogated LPS-induced histone ADP-ribosylation (Fig. 2A and B). Further analysis of the H3 and H2B bands revealed that histone H3 was most extensively modified with ADP-ribose among all four core histones (Fig. 2C). In addition, the level of [^{32}P]ADP-ribose from histone H3 immunoprecipitated by an antibody to H3 was much higher than that from histone H2B immunoprecipitated by an antibody to histone H2B, although the amounts of immunoprecipitated histones H3 and H2B were similar (Fig. 2D). The order of histone ADP-ribosylation levels in LPS-stimulated macrophages was as follows, from greatest to least: H3, H4, and H2A/B (see also Fig. 4). Together, these data demonstrate that LPS stimulation induces histone ADP-ribosylation.

LPS stimulation activates Toll-like receptor 4 (TLR4)-dependent intracellular signaling pathways, including the extracellular signal-regulated kinase (ERK) (2). Recently, ERKs have been reported to regulate PARP-1 enzymatic activity in neurons, microglia, or macrophages (10, 14). Consistent with this, pretreatment of macrophages with the MEK1/2 inhibitor UO126 blocked LPS-induced PARP-1 enzymatic activity and histone ADP-ribosylation (Fig. 3A). In contrast, UO126 did not inhibit purified PARP-1 enzymatic activity *in vitro* (Fig. 3B), and PJ34 did not inhibit LPS stimulation-induced ERK activation in macrophages (Fig. 3C). In addition, although a p38 MAPK inhibitor, SB203580, and an NF-κB inhibitor, IMD-0354, inhibited LPS stimulation-induced phosphorylation of p38 and IκB, respectively, these inhibitors did not block LPS stimulation-induced PARP-1 enzymatic activity (Fig. 3D). Therefore, these data indicate that UO126 inhibits PARP-1 enzymatic activity specifically through LPS stimulation-induced intracellular ERK pathways and suggest that PARP-1 enzymatic activity is a downstream target of the LPS stimulation-induced ERK pathway. The levels of LPS stimulation-induced pADPr-PARP-1 or ADPr-histone were not changed in cells pretreated with an antioxidant, *N*-acetylcysteine (NAC) (Fig. 3E). In addition, no single- or double-strand DNA breaks were detected by the alkaline comet assay or γH2AX Western blot analysis, respectively (Fig. 3F and G). Together, our data suggest that LPS stimulation-induced histone ADP-ribosylation is regulated through the TLR4-dependent intracellular ERK signaling path-

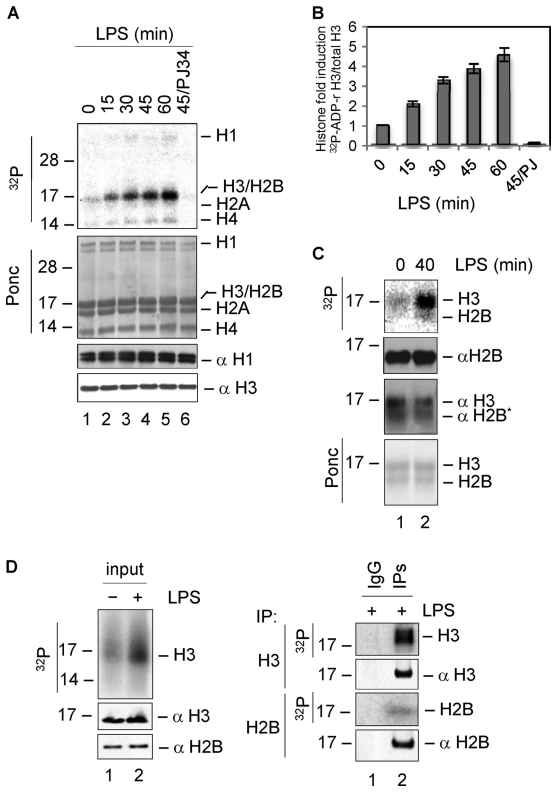

FIG 2 LPS stimulation induces histone ADP-ribosylation. (A) Macrophages were stimulated with LPS, and acid-extracted histones were processed in NuPAGE gels. [^{32}P]ADPr-histones were detected by autoradiography (A, C, and D). Ponc, Ponceau S. (B) Semiquantitative analysis of LPS stimulation-induced histone ADP-ribosylation. Fold inductions were determined as the ratio of the ^{32}P signal over histone H3 protein levels and are relative to levels in unstimulated cells (0 min). Results are from at least three independent experiments performed as described for panel A. Data are means ± standard errors of the means. (C) Acid-extracted histones from control and LPS-stimulated macrophages were separated in 16% Tris-glycine gels. Histones H3 and H2B were detected with specific antibodies. Note that H2B* in the third panel is a residual signal from the previous Western blot with an antibody to H2B. (D) Histones H3 and H2B were immunoprecipitated (IP) with antibodies to H3 or H2B from nuclear extracts of LPS-stimulated and ^{32}P-NAD$^+$-labeled macrophages.

ways, rather than resulting from DNA damage, in macrophages.

MNase-accessible chromatin regions contain ADPr-histones. We then characterized the chromatin regions containing ADPr-histones by limited MNase digestion. Four independent MNase digestions of cross-linked chromatin for 0, 1, 5, and 10 min generated nucleosome arrays, ranging from poly- to mononucleosomes, from control and LPS-stimulated macrophages after labeling with ^{32}P-NAD$^+$ (Fig. 4A, bottom). Analysis of equal amounts of digested nucleosomes showed that extensive digestion of chromatin did not increase the levels of ADPr-histones (Fig. 4A). In addition, analysis with successive MNase digestions revealed that nucleosomes containing most of the ADPr-histones were generated within 1 min of digestion. In contrast, nucleosomes generated after a 3-min digestion and the MNase-resistant chromatin fraction (P4) contained dramatically reduced levels of ADPr-histones (Fig. 4B). Therefore, both independent chromatin digestion and successive chromatin digestion suggest that most of the chromatin that is hypersensitive to nuclease digestion contains ADPr-histones. We then further analyzed nucleosome arrays generated by MNase digestion of native chromatin by sucrose gradient sedimentation. Surprisingly, gradient density analyses of nucleosome arrays revealed significant enrichment of both basal and LPS stimulation-induced ADPr-histones in the mono- and dinucleosome fractions (Fig. 4C). Together, our data demonstrate that highly accessible chromatin regions contain ADPr-histones in LPS-stimulated macrophages.

Histone ADP-ribosylation destabilizes histone-DNA interactions in the 601 nucleosome. Nucleosomes create barriers to transcription factors requiring access to DNA, and nucleosome remodeling is essential for alleviating these structural constraints so as to facilitate transcription (35, 38, 40). Given that ADP-ribose is a negatively charged molecule, histone ADP-ribosylation in mononucleosomes from LPS-stimulated macrophages (Fig. 4C) may alter local electrostatic charge density and therefore affect electrostatic interactions in the nucleosome (7). We therefore determined the effect of histone ADP-ribosylation on mononucleosome structure *in vitro*. Native gel electrophoresis showed that nucleosomes were reconstituted with the high-affinity 601 nucleosome positioning sequence and the nucleosome-bound PARP-1 complex (Fig. 5A). In addition, the naked DNA-bound PARP-1 complex was also detected with smeared bands, suggesting that the affinity of PARP-1 for naked DNA is much weaker than that for nucleosomes (Fig. 5A). Autoradiography of a NuPAGE gel revealed that all core histones were modified with ADP-ribose when PARP-1 and ^{32}P-NAD$^+$ were added to nucleosomes (Fig. 5B; also data not shown).

DNase I footprinting provides high-resolution information regarding the interaction of the DNA backbone with the core histone octamer or alterations of nucleosome structure (59). We therefore characterized the 601 nucleosome structure using DNase I digestion in the absence or presence of PARP-1 with various NAD$^+$ concentrations. The addition of PARP-1, pADPr-PARP-1, or NAD$^+$ alone to nucleosomes or naked DNA (data not shown) did not alter the DNase I digestion pattern (Fig. 5C, lane 6). However, we found that the addition of PARP-1 together with NAD$^+$ consistently altered the DNase I digestion pattern, increasing digestion in the nucleosome core particle (NCP) region specifically at positions +90, +110, +120, +140, +150, and +160 (labeled on the sense strand, relative to the 10-bp DNA ladder) (Fig. 5C, lanes 7 to 10). Importantly, the increase in DNase I sensitivity was correlated with the NAD$^+$ concentration and therefore with the extent of histone ADP-ribosylation. These data indicate that histone ADP-ribosylation perturbs histone-DNA interactions and alters the DNA path over the histone octamer.

Histone ADP-ribosylation increases the accessibility of nucleosomal DNA to nucleases. We then investigated whether changes in histone-DNA interactions by histone ADP-ribosylation could increase the accessibility of nucleosomal DNA. We therefore performed a restriction endonuclease accessibility assay using nucleosomes reconstituted with the rDNA promoter sequence, which contains two HaeIII sites (Fig. 6A, top). A small amount of cleavage products was detected in control nucleosomes, indicating that nucleosomes limit the access of HaeIII (Fig. 6A, lane 3). Surprisingly, the addition of PARP-1 and NAD$^+$ to nucleosomes increased the amount of expected cleavage products in an NAD$^+$ concentration-dependent manner (Fig. 6A, lanes 4 to 11). In contrast, the addition of PARP-1 or NAD$^+$ alone did not

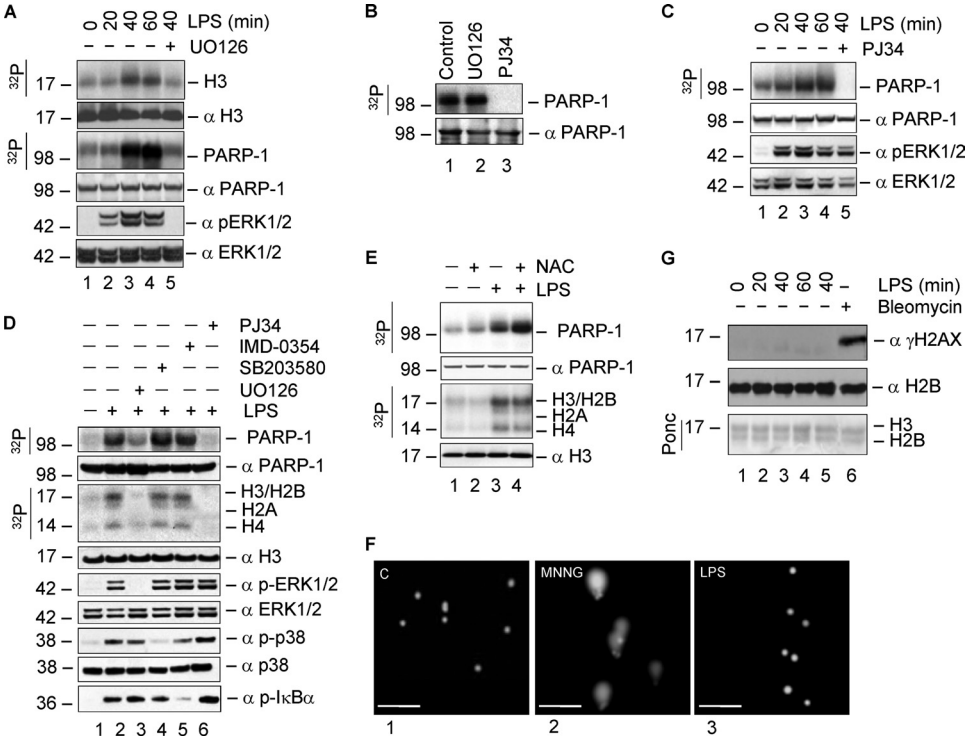

FIG 3 LPS stimulation induces histone ADP-ribosylation through an intracellular signaling pathway. (A) Cells were pretreated for 1 h with the MEK1/2 inhibitor UO126 (10 μM) (lane 5) and were then stimulated with LPS for the indicated times. ERK activation was determined by Western blot analysis with antibodies specific to phospho-ERK1/2 (A and C). Western blot analysis with antibodies to PARP-1 and total ERK1/2 shows equal protein loading (A to D). (B) Recombinant PARP-1 (100 ng) was preincubated with the MEK1/2 inhibitor UO126 (10 μM) (lane 2) and the PARP inhibitor PJ34 (lane 3) for 30 min at room temperature before the addition of ^{32}P-NAD$^+$ (100 nM). Reactions were analyzed by NuPAGE gels, autoradiography, and Western blotting. (C) Cells were pretreated with PJ34 (lane 5) for 1 h prior to LPS stimulation and were analyzed as described above. (D) RAW 264.7 macrophages were pretreated with UO126 (10 μM) (lane 3), SB203580 (10 μM) (lane 4), IMD-0354 (1 μM) (lane 5), or PJ34 (lane 6) 1 h prior to stimulation with LPS for 40 min. Activation of ERK and p38 MAPK was monitored by Western blot analysis with phospho-specific antibodies to ERK and p38 MAPK. Activation of IκK was monitored by Western blot analysis with phospho-specific antibodies to IκBα. (E) RAW 264.7 macrophages were pretreated with 1 mM *N*-acetylcysteine (NAC) for 1 h before LPS stimulation for 40 min. (F) RAW 264.7 macrophages were either left untreated (panel 1), treated with the DNA-alkylating agent *N*-methyl-*N*′-nitro-*N*-nitrosoguanidine (MNNG; 25 μM) (panel 2), or stimulated with LPS for 40 min (panel 3). Results were analyzed by the alkaline comet assay. Bars, 200 μm. (G) RAW 264.7 macrophages were either stimulated with LPS for the indicated times or treated with bleomycin (50 μg/ml) for 30 min. Acid-extracted histones were analyzed. γH2AX (top) is shown as a marker for DNA double-strand breaks. Ponc,; Ponceau S.

increase the amount of cleavage products, indicating that increased accessibility of nucleosomes was dependent on the NAD$^+$-dependent PARP-1 enzymatic activity (Fig. 6B). Similarly, increased accessibility to StyI was also observed for the 601 nucleosomes (Fig. 6C). Importantly, increased DNA accessibility persisted after PARP-1 was displaced from nucleosomes (Fig. 6C, lanes 9 and 10).

In addition to cleavage products, the addition of PARP-1 and NAD$^+$ generated naked DNA. Previously, pADPr-PARP-1 was shown to release a histone from a single histone-DNA complex (53). We therefore wanted to determine whether pADPr-PARP-1 or ADPr-histone is responsible for generating naked DNA. To this end, pADPr-PARP-1 was first prepared by incubating PARP-1 with DNA fragments and various concentrations of NAD$^+$. The addition of pADPr-PARP-1 to nucleosomes did not generate naked DNA, whereas the addition of PARP-1 with NAD$^+$, at the same concentrations used for the automodification of PARP-1, generated naked DNA (Fig. 6D). Furthermore, a highly automodified PARP-1 was unable to associate with nucleosomes (Fig. 6D). Together, these data indicate that histone ADP-ribosylation by PARP-1 is responsible for increasing the accessibility of nucleosomal DNA and altering nucleosome stability, with potential nucleosome loss.

Furthermore, the pause positions of ExoIII digestion reveal the boundary of the nucleosome position established by histone-DNA interactions at the edge of the NCP region (19). Consistent with the crystal structure of the 601 NCP (39, 58) and previous boundary mapping studies (3), ExoIII digestion revealed that the boundary of the 601 nucleosome was at positions 220 and 230 (labeled on the sense strand), approximately 73 bp away from the dyad axis. The addition of PARP-1 or NAD$^+$ alone to the nucleosome did not affect the nucleosome boundary position (Fig. 6E, lanes 3 and 4). Interestingly, we found that this boundary remained at NAD$^+$ concentrations where increased accessibility occurs (Fig. 6E), suggesting that the increased accessibility of nucleosomal DNA due to PARP-1-mediated histone ADP-ribosylation does not result from sliding of the histone octamer to a new position along the DNA. As expected, no nucleosome boundary was detected in the absence of a histone octamer (Fig. 6E, lane 9).

LPS stimulation-induced ADP-ribosylation facilitates NF-κB recruitment to the promoters and enhances transcription. To investigate the role of histone ADP-ribosylation in gene

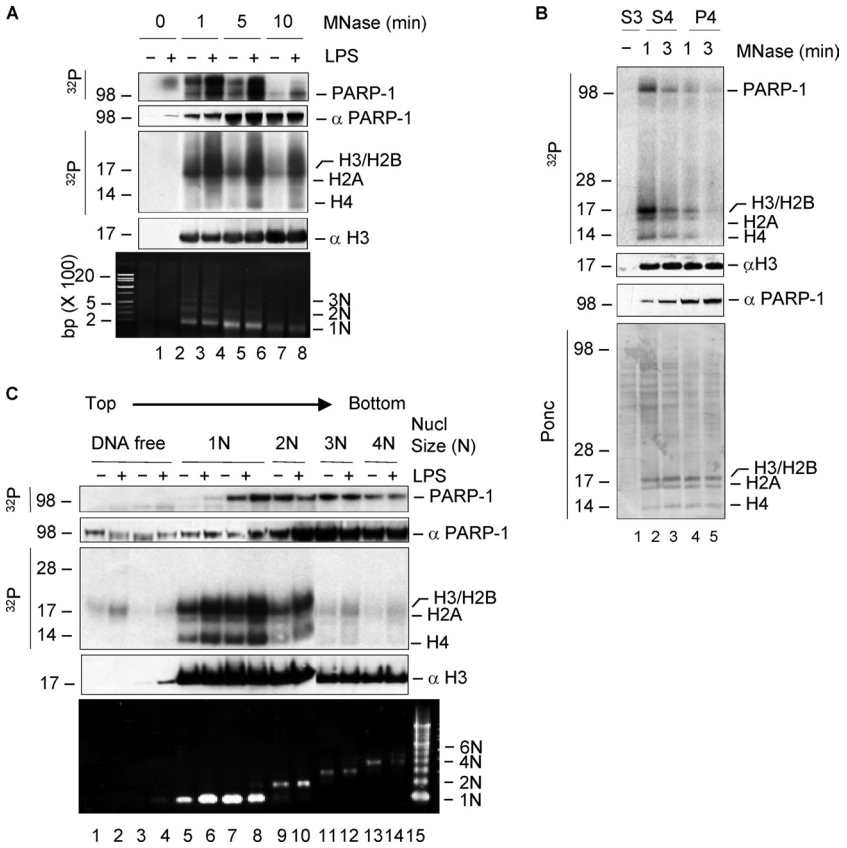

FIG 4 MNase-accessible chromatin contains ADPr-histones. (A) Control and LPS-stimulated macrophages were subjected to the PARP-1 enzymatic assay and were then immediately fixed with formaldehyde. (Top and center) Chromatin was isolated and independently digested with MNase for the indicated times, and equal amounts of protein in the solubilized chromatin fraction (S4) were analyzed. (Bottom) DNA was purified and analyzed by agarose gel electrophoresis. N, number of nucleosomes. (B) Fixed chromatin from LPS-stimulated RAW 264.7 macrophages was successively digested with MNase for the indicated times, and the soluble (S4) (lanes 2 and 3) and insoluble (P4) (lanes 4 and 5) fractions were analyzed. Equal amounts of histones from S4 and P4 fractions were analyzed. An equal amount of protein from the soluble nuclear fraction (S3) (lane 1) is shown as a specificity control for the digestion. Data in panels A and B are representative of at least three experiments. (C) Sucrose gradient analysis of nucleosomes (Nucl) containing ADPr-histones. Native chromatin was digested with MNase for 10 min, and subsequent nucleosomes were analyzed in 10-to-40% sucrose gradients in the presence of 150 mM NaCl. Equal volumes of each fraction were analyzed. Fraction numbers from the top to the bottom of the gradient (lanes 1 to 14) are given. Lane 15 contains input. Analyses of protein (top and center) and DNA (bottom) fractions are shown. N, number of nucleosomes.

transcription, we first determined the nucleosome occupancy of the promoters of a subset of inflammatory genes based on our previous study (16) and the promoters with nucleosome occupancy and the NF-κB binding site (15). Given that nucleosome occupancy and the nucleosome position can be measured by MNase digestion (31), we performed chromatin immunoprecipitation (ChIP) on MNase-digested chromatin. ChIP with antibodies to histone H3 showed that the proximal promoters of *il-1*β, *mip-2*, *csf2*, and rDNA were highly enriched with histone H3 relative to those of β-*actin* and *brca1* in both resting and LPS-stimulated macrophages, indicating that nucleosomes occupy these regions (Fig. 7A). Recently, PARP-1 has been suggested to promote transcription by binding at the promoters of genes (25, 29). Consistent with this, ChIP with an antibody to PARP-1 showed enrichment at the proximal promoters of *il-1*β, *mip-2*, and *csf2* (Fig. 7B), suggesting that PARP-1 is associated with nucleosomes at these promoters. Interestingly, PARP-1 was not detected, and the level of histone H3 was reduced, at the promoter of *csf2* after LPS stimulation (Fig. 7B), suggesting that highly automodified PARP-1 could be displaced from this promoter region, with possible nucleosome loss, in response to LPS stimulation (Fig. 1G). We then determined the levels of local ADP-ribosylation at these promoters after LPS stimulation. Biotin-conjugated NAD^+ was previously shown to detect pADPr-protein(s) in polytene chromosome regions in *Drosophila* larval salivary glands (57). Consistent with the results from limited MNase digestions (Fig. 4B), we found that pADPr-PARP-1 and ADPr-histones were the major species selectively and specifically purified by streptavidin agarose beads from the chromatin of macrophages colabeled with biotinylated NAD^+ and ^{32}P-NAD^+ (data not shown). Further ChIP analyses revealed that ADP-ribose was synthesized at the promoters of *il-1*β, *mip-2*, and *csf2* in an LPS stimulation-dependent manner, and the level of ADP-ribose was increased in a time-dependent manner (Fig. 7C). In contrast, ADP-ribose synthesis was not detected at the promoters of *brca1* and β-*actin* (Fig. 7C). In addition, despite the presence of nucleosomes at the rDNA promoter (33, 65), ADP-ribose synthesis was not detected at this promoter. As expected, the addition of PJ34 abrogated ADP-ribose synthesis at the *il-1*β, *mip-2*, and *csf2* promoters (Fig. 7C).

Regulation of promoter chromatin structure was recently

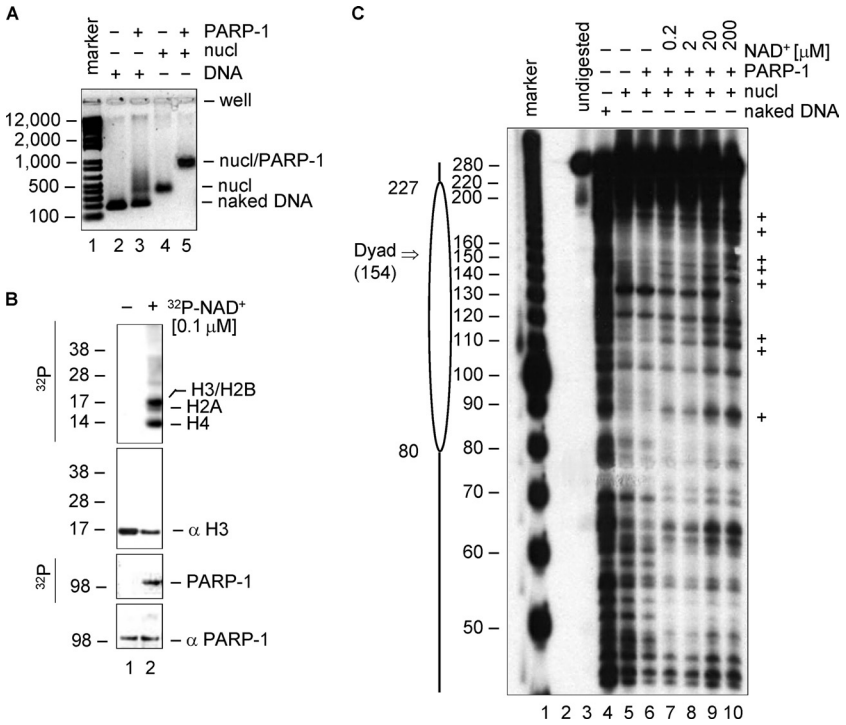

FIG 5 Histone ADP-ribosylation directly alters nucleosome structure. (A) PARP-1 was incubated in the presence of equal molar amounts of naked DNA (lane 3) or reconstituted 601 nucleosomes (lane 5), and the binding complex was analyzed by native agarose gel electrophoresis followed by visualization in a UV transilluminator after SYBR green staining of DNA. Naked DNA (lane 2), naked DNA with PARP-1 (lane 3), reconstituted nucleosomes (lane 4), and the PARP-1/nucleosome complex (lane 5) are shown. nucl, nucleosomes. (B) The 601 nucleosomes were incubated with PARP-1 in the presence or absence of 100 nM ^{32}P-NAD$^+$, and protein was analyzed by NuPAGE gels, autoradiography, and Western blotting. (C) The 601 nucleosomes labeled with ^{32}P at the 5′ end of the sense strand were incubated with PARP-1 and with NAD$^+$ at the indicated concentrations (lanes 6 to 10). Reactions were analyzed in 8% denaturing polyacrylamide gels followed by autoradiography. +, DNase I-hypersensitive sites. Lane 1, DNA marker; lane 2, empty; lanes 3 and 4, undigested and digested DNA controls; lane 5, control nucleosomes.

shown to be important for promoting NF-κB-dependent inflammatory gene transcription (13, 43, 44, 54), and our data showed that histone ADP-ribosylation increased the accessibility of nucleosomal DNA. We therefore hypothesized that histone ADP-ribosylation might enhance the recruitment of NF-κB to nucleosome-occupied promoters of these genes. We therefore determined the effect of LPS stimulation-induced ADP-ribose on NF-κB recruitment by performing ChIP with an antibody to the p65 subunit of NF-κB in macrophages. We found that p65 was recruited to the promoters of *il-1*β, *mip-2*, and *csf2* in an LPS stimulation-dependent manner (Fig. 7D). Surprisingly, pretreatment of cells with PJ34 significantly reduced the LPS stimulation-induced recruitment of p65 to these promoters (Fig. 7D), suggesting that changes in DNA accessibility due to a PARP inhibitor limit the interaction between p65 and its binding sites. Together, these data suggest that LPS stimulation-induced ADP-ribosylation at the promoter facilitates the recruitment of p65 to its consensus site.

To assess the effect of reduced p65 recruitment due to a PARP inhibitor, we determined the transcription of these inflammatory genes. Quantitative real-time PCR analyses revealed that LPS stimulation induced the expression of *il-1*β, *mip-2*, and *csf2* in a time-dependent manner in macrophages. Consistent with reduced p65 recruitment, pretreatment of macrophages with PJ34 showed that LPS stimulation-induced expression of these genes was impaired (Fig. 7E). Furthermore, LPS stimulation-induced expression of interleukin 1β (IL-1β) was impaired in PARP-1-deficient cells (Fig. 7F), suggesting that the transcriptional outcome of these genes is directly mediated by PARP-1. Together, these data suggest that LPS stimulation-induced ADP-ribosylation facilitates p65 recruitment to its consensus site at the promoters of *il-1*β, *mip-2*, and *csf2*, as well as the transcription of these genes.

DISCUSSION

Since its initial discovery in 1963 (9), the ADP-ribose polymer has been firmly established as a posttranslational protein modifier. Here we showed for the first time that LPS stimulation induced PARP-1 enzymatic activity and histone ADP-ribosylation through a TLR4-dependent intracellular signaling pathway. Importantly, histone ADP-ribosylation increased DNA accessibility and facilitated efficient transcription of a subset of LPS stimulation-inducible genes in macrophages.

Previous studies have shown that inhibition of PARP-1 enzymatic activity or deletion of PARP-1 impairs the expression of NF-κB-dependent inflammatory cytokines in response to various inflammatory stimuli (17, 20, 24, 42, 45). Notably, PARP inhibitors have been shown to reduce the LPS stimulation-induced expression of macrophage inflammatory protein 1α (MIP-1α) and MIP-2 in murine macrophages (20) and of tumor necrosis factor alpha (TNF-α), IL-6, IL-1β, and inducible nitric oxide synthase (iNOS) in primary glial cells (17, 42). Furthermore, PARP-1 en-

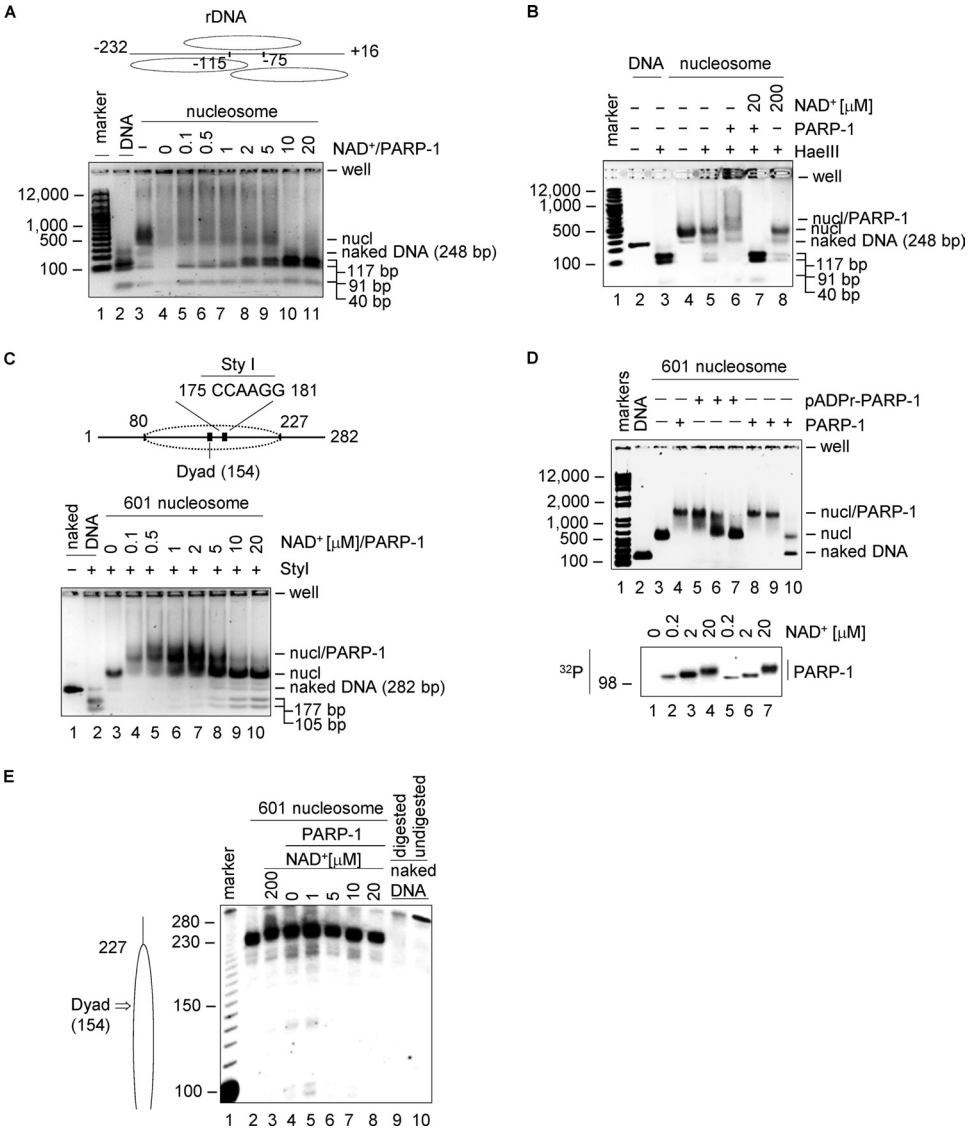

FIG 6 Histone ADP-ribosylation increases the accessibility of nucleosomal DNA. (A to C) Nucleosomes assembled with the rDNA promoter sequence (A and B) or the 601 nucleosomes (C) were incubated with PARP-1 and the indicated NAD^+ concentrations (A to C) or 200 μM NAD^+ alone (B, lane 8) as indicated. Subsequent nucleosomes were digested with HaeIII (A and B) or StyI (C) for 1.5 h at 37°C. Reactions were analyzed in 1.7% agarose gels. Schematic representations of the HaeIII and StyI sites in the assembled nucleosomes are shown at the tops of panels A and C. (D) (Top) The addition of purified pADPr-PARP-1, automodified with 0.2, 2, or 20 μM NAD^+ (lanes 5 to 7, respectively), to nucleosomes did not generate naked DNA, whereas the addition of PARP-1 with 0.2, 2, or 20 μM NAD^+ (lanes 8 to 10) to nucleosomes did generate naked DNA. The addition of PARP-1 without NAD^+ is shown in lane 4. (Bottom) The extent of poly(ADP-ribosyl)ation of PARP-1 was determined by autoradiography. Lanes 2 to 4, pADPr-PARP-1 before any addition to nucleosomes; lanes 5 to 7, pADPr-PARP-1 during incubation of PARP-1 and NAD^+ with nucleosomes. (E) The nucleosome position boundary (relative to the sense strand) was mapped by ExoIII digestion. Nucleosomes in the absence of PARP-1 (lane 2) and in the presence of 200 μM NAD^+ alone (lane 3) are shown. Data in all panels are representative of at least three experiments.

zymatic activity has been suggested to exchange repression complexes containing histone H1 for activation complexes containing HMGB1/2 by the ADP-ribosylation of H1, causing H1 release from the nucleosome positioned in the *pS2* promoter region (25). A PARP inhibitor has been shown to block this exchange of H1 with HMGB1/2 and, in turn, inhibits *pS2* gene transcription (25). In addition, the ADP-ribose polymer has been shown to accumulate at puffing sites and the *Hsp70* locus in *Drosophila melanogaster* (57). Furthermore, puffing is absent, and the level of *Hsp70* gene transcription is reduced, in cells treated with a PARP inhibitor or expressing a mutant PARP, suggesting that synthesis of the ADP-ribose polymer is required for puff formation and the full transcription of the *Hsp70* gene (57). In addition, ADP-ribosylation was recently implicated in nucleosome loss in the *Hsp70* locus independently of gene transcription, since a PARP inhibitor or deletion of PARP by RNA interference (RNAi) blocked nucleosome loss and reduced *Hsp70* gene transcription in *Drosophila* (49). The ADP-ribosylation of nucleosomal histones and/or the pADPr-PARP-1 associated with the nucleosomes positioned at the *Hsp70* gene are conjectured to be associated with nucleosome loss (49). Furthermore, biochemical and electron microscopy studies with isolated polynucleosomes suggest that PARP-1 may

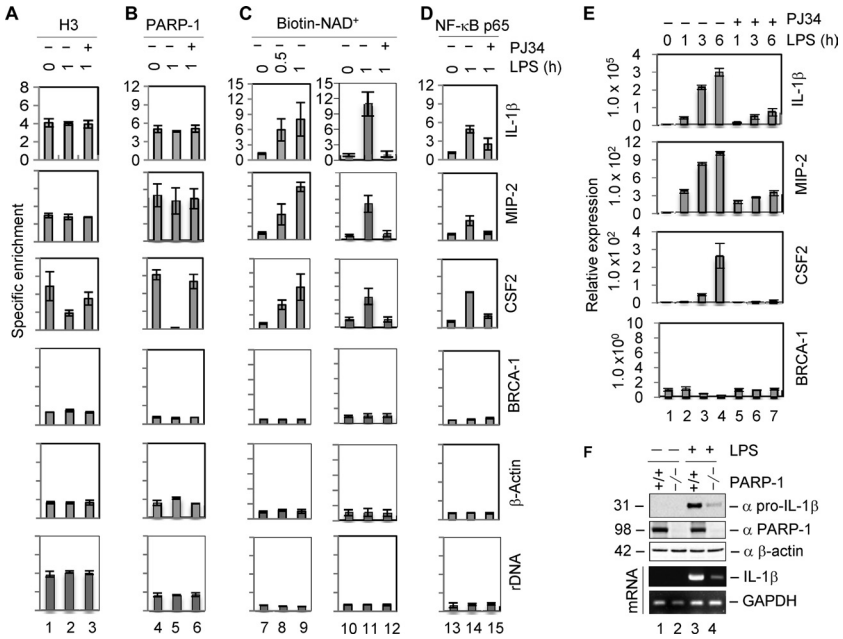

FIG 7 LPS stimulation-induced ADP-ribosylation facilitates gene transcription in macrophages. (A to D) ChIP analyses of histone H3 (A), PARP-1 (B), ADP-ribose (C), and NF-κB p65 (D) at the promoters of the indicated genes in control and LPS-stimulated macrophages with or without pretreatment with PJ34. (E) Macrophages either were left untreated or were treated with PJ34; then they were stimulated with LPS. Total RNA was extracted, and the mRNA levels of the indicated genes were measured by quantitative real-time PCR. Relative expression was determined as the ratio of the mRNA levels of genes to the mRNA levels of β-actin and is relative to expression in unstimulated cells (0 h). Data are means ± standard errors of the means. (F) The expression of IL-1β was measured in PARP-1-deficient and normal cells stimulated with LPS for 3 h.

decondense chromatin structure by the poly(ADP-ribosyl)ation of histone H1 (50). In addition, pADPr-PARP-1 or ADP-ribose polymer has been shown to interact strongly with individual histones and to disrupt the interaction of a single histone with nucleosomal DNA (47, 53). Although PARP inhibitors implicate PARP enzymatic activity in gene transcription, its targets, including ADP-ribosylation of histones, have not been identified.

In this report, we showed that the primary targets of ADP-ribosylation in LPS-stimulated macrophages were PARP-1 itself, but not PARP-2, and all four core histones. Activation of the PARP enzyme is indicated by automodification (24), and therefore, our data suggest that within the PARP family, LPS stimulation-induced PARP-1 is the enzyme that targets histones. In line with these data, we found that purified PARP-1, rather than PARP-2, mainly modified histones of reconstituted nucleosomes *in vitro* (data not shown), indicating that PARP-1 may be the main cellular enzyme that targets chromatin. Therefore, although PARP inhibitors lack the specificity to determine which PARP enzyme is relevant to facilitating gene expression, studies on PARP-1-deficient cells (Fig. 7F) and on mice (17, 46), and our data on LPS stimulation-induced PARP-1 enzymatic activity (Fig. 1), suggest that PARP-1 enzymatic activity is the most relevant target of PJ34 in LPS-stimulated macrophages. Even though we did not detect other ADPr-chromatin-related proteins in response to LPS stimulation, we cannot rule out the possibility that other proteins could be also modified with ADP-ribose. Notably, basal PARP-1 enzymatic activity was detected in macrophages. Given that PARP-1 is also shown to regulate LPS-independent gene transcription (10, 25), including basal gene transcription (29, 30), it is possible that histone ADP-ribosylation can also occur at the promoter regions of genes to regulate basal gene transcription independently of LPS stimulation in macrophages.

Our ChIP analyses with MNase-digested chromatin showed that promoter regions of *il-1*β, *mip-2*, and *csf2*, containing the p65 binding site, were occupied with nucleosomes, although the precise nucleosome positions in these promoters have not yet been determined. Furthermore, ChIP analyses revealed that PARP-1 was constitutively associated with these regions, suggesting that PARP-1 could facilitate gene transcription epigenetically in response to environmental cues. Importantly, LPS stimulation-induced ADP-ribosylation at these promoters is closely correlated with enhanced recruitment of the p65 subunit of NF-κB and increased transcription. Given that the nucleosome is the primary determinant of DNA accessibility (6), these data suggest that nucleosomes at these promoters could limit the access of p65, and possibly other transcription factors and regulators, to its consensus site and that histone ADP-ribosylation could alleviate these obstacles so as to facilitate transcription. Both PARP-1 and nucleosomal histones were likely ADP-ribosylated at these promoters in macrophages. It is currently unknown whether PARP-1 at these promoters has additional roles besides histone ADP-ribosylation. However, we cannot rule out the possibility that other targets, including the recruitment of transcription regulators, are equally important for facilitating gene transcription, since PARP-1 is known to interact with other factors, such as ATP-dependent chromatin-remodeling factors (1, 41) (in a PARP-1 enzymatic activity-dependent manner) or NF-κB (21) (in a PARP-1 enzymatic activity-independent manner). In this report, *in vitro* DNase I digestion and restriction endonuclease accessibility studies suggest that histone ADP-ribosylation is responsible for

increasing the accessibility of nucleosomal DNA by modulating histone-DNA interactions in the nucleosome. Therefore, histone ADP-ribosylation could facilitate enhanced p65 binding to the promoters of *il-1*β, *mip-2*, and *csf2* and the transcription of these genes in LPS-stimulated macrophages.

ChIP analyses showed that LPS stimulation-induced ADP-ribose synthesis correlated with a reduction in nucleosome occupancy and PARP-1 levels in the *csf2* promoter but not in the *il-1*β or *mip-2* promoter. The generation of naked DNA in the *in vitro* nucleosome-remodeling assay (Fig. 6) suggests that the increased levels and/or sites of histone ADP-ribosylation, i.e., the size of the ADP-ribose polymer and the total number of ADP-ribosylated sites within the nucleosome, could have a cumulative structural effect on the nucleosome. Accumulation of a negative charge could drastically alter the electrostatic interactions of histones and DNA, leading to nucleosome loss by the displacement of ADPr-histones from DNA through the repulsive electrostatic force at the promoter regions. Consistent with this notion, we also found that a highly automodified PARP-1 enzyme was displaced from nucleosomes (Fig. 6). Alternatively, nucleosomes in the *il-1*β and *mip-2* promoters may be more stable than those in the *csf-2* promoter, since nucleosome stability can be regulated by the relative affinity of promoter sequences for the histone octamer (51). In addition, the extent of nucleosome remodeling could be affected by the rotational and translational positions of the NF-κB site in the nucleosome (44). Further studies mapping the precise nucleosome positions at these promoters will provide the extent of nucleosome remodeling required for efficient gene transcription.

Interestingly, the ExoIII digestion study showed that nucleosome remodeling by histone ADP-ribosylation did not involve histone octamer sliding along DNA. This indicates that NAD^+-dependent nucleosome remodeling is mechanistically distinct from ATP-dependent chromatin-remodeling complexes, which slide the histone octamer along DNA after modulating histone-DNA interactions (8). Furthermore, DNase I-hypersensitive sites in the nucleosome were consistent in a number of repeated experiments, suggesting that specific sites of histone ADP-ribosylation lead to specific nucleosome structure changes. Therefore, identification of the target amino acids of histone ADP-ribosylation in the nucleosome will further illuminate the molecular mechanisms by which histone ADP-ribosylation alters histone-DNA interactions. Based on its ability to alter histone-DNA interactions in the NCP region, the modification site(s) is likely located in the globular region of histone, since the acetylation of N-terminal tails does not alter individual nucleosome structure (5).

The precise size of ADP-ribose has yet to be determined in LPS-stimulated cells. However, the mobility of ADPr-histones in our gel analyses suggests that histone ADP-ribosylation consists mostly of mono(ADP-ribose), with some oligo(ADP-ribose), whereas PARP-1 ADP-ribosylation consists mainly of poly(ADP-ribose), which was also detected by antibodies to poly(ADP-ribose) with the specificity range of 6 to 100 ADPr units (Fig. 1C). In contrast to the findings for cellular ADP-ribosylation, an *in vitro* PARP assay showed that histone ADP-ribosylation was mostly polymeric, since the concentration of NAD^+ was increased, and the mobility of ADPr-histones was greatly reduced, with smeared bands, reflecting the heterogeneity of the ADP-ribose polymer. Under these conditions, histone poly(ADP-ribosyl)ation could lead to a more drastic change in nucleosome structure.

Interestingly, our data show that LPS stimulation-induced histone ADP-ribosylation is enriched in the chromatin regions that are highly sensitive to MNase digestion. Furthermore, sucrose gradient analyses of nucleosome arrays generated by MNase digestion showed that mono- and dinucleosome fractions were enriched with ADPr-histones but not with the linker histone H1. The linker histone H1 is known to be a main target of ADP-ribosylation in response to DNA damage (12, 28). However, our data showed that the linker histone H1 was not targeted by ADP-ribosylation in LPS-stimulated cells. Together, these data suggest that LPS stimulation-induced histone ADP-ribosylation occurs readily at MNase-accessible chromatin regions where histone H1 is not enriched. These data are in line with a recent analysis of the genomewide distribution of PARP-1 (29), which shows that the chromatin occupancy of PARP-1 is mutually exclusive with that of histone H1. Further study is required to determine whether PARP-1 is mutually exclusive with H1 throughout the whole genome in macrophages, including MNase-inaccessible chromatin regions where H1 modulates the higher-order chromatin structure.

Inhibition of PARP enzymatic activity did not affect LPS stimulation-induced activation of ERK. In addition, activation of NF-κB, including phosphorylation and degradation of IκB and subsequent p65 nuclear translocation, has been shown to be normal in PARP-1-deficient animals (46). Together, these data indicate that the repressive effect of a PARP inhibitor on transcription likely occurs at the chromatin level rather than affecting TLR4-dependent intracellular signaling in the cytoplasm. In addition, our data are consistent with recently emerging evidence that regulation of chromatin structure is an important determinant of NF-κB-mediated inflammatory gene expression (43, 44). Distinct patterns of TLR4-induced chromatin modifications have been shown to occur in the tolerizable and nontolerizable gene classes in macrophages (15). Furthermore, chromatin modifications at the promoter region have been shown to provide an additional regulatory mechanism for the gene-specific inflammatory response in macrophages, including the phosphorylation of histone H3S10 (54), the demethylation of trimethylated H3K27 (13), and the ubiquitylation of histone H2AK119 (64).

Collectively, our findings identify and establish PARP-1 as a poly(ADP-ribose)-dependent chromatin-modifying and -remodeling enzyme, functionally and mechanistically different from any known histone modifications or ATP-dependent chromatin -remodeling for regulating gene transcription. Given that PARP-1 enzymatic activity is also regulated by other transcriptional stimuli (10, 14, 25, 26), our findings suggest that histone ADP-ribosylation-dependent nucleosome remodeling may be a widely used mechanism to facilitate inducible gene transcription. Furthermore, our data suggest that histone ADP-ribosylation-dependent nucleosome remodeling may also play roles in other chromatin-dependent processes, including DNA replication and repair, where PARP enzymatic activity has been known to occur (22).

ACKNOWLEDGMENTS

We thank Jonathan Widom for the 601 clone and the information on the site exposure assay. In addition, we thank Stephen T. Smale, Robert A. Casero, Jr., Kevin T. FitzGerald, and members of H. C. Ha's lab for critical reading of the manuscript.

R.M.-Z. is supported by a fellowship grant from the National Council

on Science and Technology (CONACyT) of the government of Mexico. This work was supported by Public Health Service grants AI64706 and AI059678 from the National Institutes of Health.

REFERENCES

1. **Ahel D, et al.** 2009. Poly(ADP-ribose)-dependent regulation of DNA repair by the chromatin remodeling enzyme ALC1. Science **325**:1240–1243.
2. **Akira S, Takeda K.** 2004. Toll-like receptor signalling. Nat. Rev. Immunol. **4**:499–511.
3. **Anderson JD, Widom J.** 2000. Sequence and position-dependence of the equilibrium accessibility of nucleosomal DNA target sites. J. Mol. Biol. **296**:979–987.
4. **Bannister AJ, Kouzarides T.** 2011. Regulation of chromatin by histone modifications. Cell Res. **21**:381–395.
5. **Bauer WR, Hayes JJ, White JH, Wolffe AP.** 1994. Nucleosome structural changes due to acetylation. J. Mol. Biol. **236**:685–690.
6. **Bell O, Tiwari VK, Thoma NH, Schubeler D.** 2011. Determinants and dynamics of genome accessibility. Nat. Rev. Genet. **12**:554–564.
7. **Boulikas T.** 1992. Poly(ADP-ribose) synthesis and degradation in mammalian nuclei. Anal. Biochem. **203**:252–258.
8. **Cairns BR.** 2007. Chromatin remodeling: insights and intrigue from single-molecule studies. Nat. Struct. Mol. Biol. **14**:989–996.
9. **Chambon P, Weill JD, Mandel P.** 1963. Nicotinamide mononucleotide activation of new DNA-dependent polyadenylic acid synthesizing nuclear enzyme. Biochem. Biophys. Res. Commun. **11**:39–43.
10. **Cohen-Armon M, et al.** 2007. DNA-independent PARP-1 activation by phosphorylated ERK2 increases Elk1 activity: a link to histone acetylation. Mol. Cell **25**:297–308.
11. **D'Amours D, Desnoyers S, D'Silva I, Poirier GG.** 1999. Poly(ADP-ribosyl)ation reactions in the regulation of nuclear functions. Biochem. J. **342**(Pt 2):249–268.
12. **de Murcia G, Huletsky A, Poirier GG.** 1988. Modulation of chromatin structure by poly(ADP-ribosyl)ation. Biochem. Cell Biol. **66**:626–635.
13. **De Santa F, et al.** 2007. The histone H3 lysine-27 demethylase Jmjd3 links inflammation to inhibition of polycomb-mediated gene silencing. Cell **130**:1083–1094.
14. **Farez MF, et al.** 2009. Toll-like receptor 2 and poly(ADP-ribose) polymerase 1 promote central nervous system neuroinflammation in progressive EAE. Nat. Immunol. **10**:958–964.
15. **Foster SL, Hargreaves DC, Medzhitov R.** 2007. Gene-specific control of inflammation by TLR-induced chromatin modifications. Nature **447**:972–978.
16. **Ha HC.** 2004. Defective transcription factor activation for proinflammatory gene expression in poly(ADP-ribose) polymerase 1-deficient glia. Proc. Natl. Acad. Sci. U. S. A. **101**:5087–5092.
17. **Ha HC, Hester LD, Snyder SH.** 2002. Poly(ADP-ribose) polymerase-1 dependence of stress-induced transcription factors and associated gene expression in glia. Proc. Natl. Acad. Sci. U. S. A. **99**:3270–3275.
18. **Hamiche A, Kang JG, Dennis C, Xiao H, Wu C.** 2001. Histone tails modulate nucleosome mobility and regulate ATP-dependent nucleosome sliding by NURF. Proc. Natl. Acad. Sci. U. S. A. **98**:14316–14321.
19. **Hamiche A, Sandaltzopoulos R, Gdula DA, Wu C.** 1999. ATP-dependent histone octamer sliding mediated by the chromatin remodeling complex NURF. Cell **97**:833–842.
20. **Hasko G, et al.** 2002. Poly(ADP-ribose) polymerase is a regulator of chemokine production: relevance for the pathogenesis of shock and inflammation. Mol. Med. **8**:283–289.
21. **Hassa PO, Buerki C, Lombardi C, Imhof R, Hottiger MO.** 2003. Transcriptional coactivation of nuclear factor-κB-dependent gene expression by p300 is regulated by poly(ADP)-ribose polymerase-1. J. Biol. Chem. **278**:45145–45153.
22. **Jackson SP, Bartek J.** 2009. The DNA-damage response in human biology and disease. Nature **461**:1071–1078.
23. **Jacobson RH, Ladurner AG, King DS, Tjian R.** 2000. Structure and function of a human TAFII250 double bromodomain module. Science **288**:1422–1425.
24. **Jagtap P, Szabo C.** 2005. Poly(ADP-ribose) polymerase and the therapeutic effects of its inhibitors. Nat. Rev. Drug Discov. **4**:421–440.
25. **Ju BG, et al.** 2006. A topoisomerase IIβ-mediated dsDNA break required for regulated transcription. Science **312**:1798–1802.
26. **Ju BG, et al.** 2004. Activating the PARP-1 sensor component of the Groucho/TLE1 corepressor complex mediates a CaMKinase IIδ-dependent neurogenic gene activation pathway. Cell **119**:815–829.
27. **Kouzarides T.** 2007. Chromatin modifications and their function. Cell **128**:693–705.
28. **Kreimeyer A, Wielckens K, Adamietz P, Hilz H.** 1984. DNA repair-associated ADP-ribosylation in vivo. Modification of histone H1 differs from that of the principal acceptor proteins. J. Biol. Chem. **259**:890–896.
29. **Krishnakumar R, et al.** 2008. Reciprocal binding of PARP-1 and histone H1 at promoters specifies transcriptional outcomes. Science **319**:819–821.
30. **Krishnakumar R, Kraus WL.** 2010. PARP-1 regulates chromatin structure and transcription through a KDM5B-dependent pathway. Mol. Cell **39**:736–749.
31. **Landsberger N, Wolffe AP.** 1997. Remodeling of regulatory nucleoprotein complexes on the *Xenopus* hsp70 promoter during meiotic maturation of the *Xenopus* oocyte. EMBO J. **16**:4361–4373.
32. **Langst G, Becker PB.** 2001. ISWI induces nucleosome sliding on nicked DNA. Mol. Cell **8**:1085–1092.
33. **Langst G, Schatz T, Langowski J, Grummt I.** 1997. Structural analysis of mouse rDNA: coincidence between nuclease hypersensitive sites, DNA curvature and regulatory elements in the intergenic spacer. Nucleic Acids Res. **25**:511–517.
34. **Li B, Carey M, Workman JL.** 2007. The role of chromatin during transcription. Cell **128**:707–719.
35. **Lorch Y, Maier-Davis B, Kornberg RD.** 2006. Chromatin remodeling by nucleosome disassembly in vitro. Proc. Natl. Acad. Sci. U. S. A. **103**:3090–3093.
36. **Lorch Y, Zhang M, Kornberg RD.** 1999. Histone octamer transfer by a chromatin-remodeling complex. Cell **96**:389–392.
37. **Lowary PT, Widom J.** 1998. New DNA sequence rules for high affinity binding to histone octamer and sequence-directed nucleosome positioning. J. Mol. Biol. **276**:19–42.
38. **Luk E, et al.** 2010. Stepwise histone replacement by SWR1 requires dual activation with histone H2A.Z and canonical nucleosome.Cell **143**:725–736.
39. **Makde RD, England JR, Yennawar HP, Tan S.** 2010. Structure of RCC1 chromatin factor bound to the nucleosome core particle. Nature **467**:562–566.
40. **Mizuguchi G, et al.** 2004. ATP-driven exchange of histone H2AZ variant catalyzed by SWR1 chromatin remodeling complex. Science **303**:343–348.
41. **Murawska M, Hassler M, Renkawitz-Pohl R, Ladurner A, Brehm A.** 2011. Stress-induced PARP activation mediates recruitment of *Drosophila* Mi-2 to promote heat shock gene expression. PLoS Genet. **7**:e1002206. doi:10.1371/journal.pgen.1002206.
42. **Nakajima H, et al.** 2004. Critical role of the automodification of poly-(ADP-ribose) polymerase-1 in nuclear factor-κB-dependent gene expression in primary cultured mouse glial cells. J. Biol. Chem. **279**:42774–42786.
43. **Natoli, G.** 2009. Control of NF-κB-dependent transcriptional responses by chromatin organization. Cold Spring Harb. Perspect. Biol. **1**:a000224. doi:10.1101/cshperspect.a000224.
44. **Natoli G, Saccani S, Bosisio D, Marazzi I.** 2005. Interactions of NF-κB with chromatin: the art of being at the right place at the right time. Nat. Immunol. **6**:439–445.
45. **Nirodi C, et al.** 2001. A role for poly(ADP-ribose) polymerase in the transcriptional regulation of the melanoma growth stimulatory activity (CXCL1) gene expression. J. Biol. Chem. **276**:9366–9374.
46. **Oliver FJ, et al.** 1999. Resistance to endotoxic shock as a consequence of defective NF-κB activation in poly(ADP-ribose) polymerase-1 deficient mice. EMBO J. **18**:4446–4454.
47. **Panzeter PL, et al.** 1993. Targeting of histone tails by poly(ADP-ribose). J. Biol. Chem. **268**:17662–17664.
48. **Peterson CL, Laniel MA.** 2004. Histones and histone modifications. Curr. Biol. **14**:R546–R551.
49. **Petesch SJ, Lis JT.** 2008. Rapid, transcription-independent loss of nucleosomes over a large chromatin domain at Hsp70 loci. Cell **134**:74–84.
50. **Poirier GG, de Murcia G, Jongstra-Bilen J, Niedergang C, Mandel P.** 1982. Poly(ADP-ribosyl)ation of polynucleosomes causes relaxation of chromatin structure. Proc. Natl. Acad. Sci. U. S. A. **79**:3423–3427.
51. **Ramirez-Carrozzi VR, et al.** 2009. A unifying model for the selective

regulation of inducible transcription by CpG islands and nucleosome remodeling. Cell **138**:114–128.
52. **Ransom M, Dennehey BK, Tyler JK.** Chaperoning histones during DNA replication and repair. Cell **140**:183–195.
53. **Realini CA, Althaus FR.** 1992. Histone shuttling by poly(ADP-ribosylation). J. Biol. Chem. **267**:18858–18865.
54. **Saccani S, Pantano S, Natoli G.** 2002. p38-Dependent marking of inflammatory genes for increased NF-κB recruitment. Nat. Immunol. **3**:69–75.
55. **Shogren-Knaak M, et al.** 2006. Histone H4–K16 acetylation controls chromatin structure and protein interactions. Science **311**:844–847.
56. **Szabo C, et al.** 1997. Inhibition of poly(ADP-ribose) synthetase attenuates neutrophil recruitment and exerts antiinflammatory effects. J. Exp. Med. **186**:1041–1049.
57. **Tulin A, Spradling A.** 2003. Chromatin loosening by poly(ADP)-ribose polymerase (PARP) at *Drosophila* puff loci. Science **299**:560–562.
58. **Vasudevan D, Chua EY, Davey CA.** 2010. Crystal structures of nucleosome core particles containing the '601' strong positioning sequence. J. Mol. Biol. **403**:1–10.
59. **Vitolo JM, Thiriet C, Hayes JJ.** 2001. DNase I and hydroxyl radical characterization of chromatin complexes. Curr. Protoc. Mol. Biol. 2001: Chapter 21:Unit 21.4. doi:10.1002/0471142727.mb2104s48.
60. **Workman JL, Kingston RE.** 1998. Alteration of nucleosome structure as a mechanism of transcriptional regulation. Annu. Rev. Biochem. **67**:545–579.
61. **Wysocka J, Reilly PT, Herr W.** 2001. Loss of HCF-1-chromatin association precedes temperature-induced growth arrest of tsBN67 cells. Mol. Cell. Biol. **21**:3820–3829.
62. **Wysocka J, et al.** 2005. WDR5 associates with histone H3 methylated at K4 and is essential for H3 K4 methylation and vertebrate development. Cell **121**:859–872.
63. **Wysocka J, et al.** 2006. A PHD finger of NURF couples histone H3 lysine 4 trimethylation with chromatin remodelling. Nature **442**:86–90.
64. **Zhou W, et al.** 2008. Histone H2A monoubiquitination represses transcription by inhibiting RNA polymerase II transcriptional elongation. Mol. Cell **29**:69–80.
65. **Zhou Y, Santoro R, Grummt I.** 2002. The chromatin remodeling complex NoRC targets HDAC1 to the ribosomal gene promoter and represses RNA polymerase I transcription. EMBO J. **21**:4632–4640.